

Supplementary information for: Detailed study of interphase degradation in SiC/BN/SiC ceramic matrix composites after elevated temperature tensile testing

L. R. M. Toller-Nordström^{a,*}, O. Gavalda-Diaz^b, L. Gale^c, D. E. J. Armstrong^a, R. J. Nicholls^{a,*}

^a*Department of Materials, University of Oxford, Oxford OX1 3PH, UK*

^b*Department of Materials, Imperial College London, London SW7 2AC, UK*

^c*Rolls Royce plc., Derby DE24 8BJ, UK*

Abstract

Ceramic matrix composites of silicon carbide fibres in a silicon carbide matrix with boron nitride interphase are promising candidates for replacing super-alloys in the hottest part of aerospace engines, reducing the need for cooling and increasing the fuel efficiency. This needs a thorough understanding of how these materials degrade under high levels of stress combined with high temperatures in an oxidative environment. This work presents a detailed investigation of the degradation in the interphase and surrounding interfaces. Advanced electron microscopy and electron energy loss spectroscopy are used to extract information on the degradation process. It was found that silica and boria form along with a migration of silica into the interphase. At 1000 °C the degradation along the surface leads to early fracture at the surface and eventually complete fracture of the composite, lower temperature allows for the oxidation to reach the centre of the sample before complete failure.

*Corresponding authors

Email addresses: lisa.toller-nordstrom@materials.ox.ac.uk (L. R. M. Toller-Nordström), rebecca.nicholls@materials.ox.ac.uk (R. J. Nicholls)

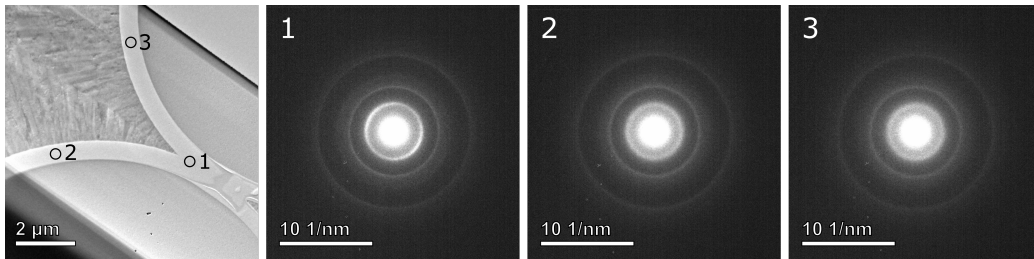


Figure 1: Diffraction patterns from the interphase in the sample CMC1000.

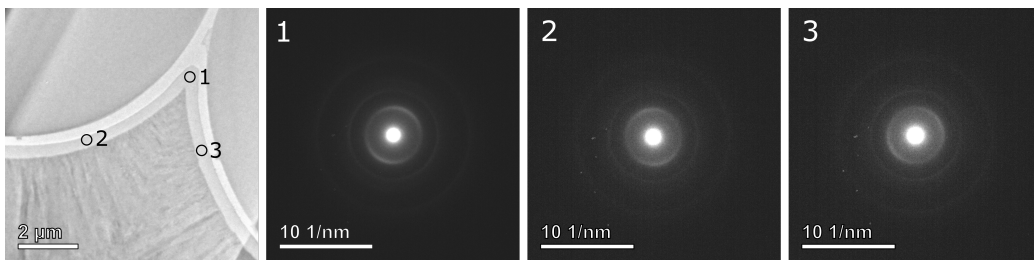


Figure 2: Diffraction patterns from the interphase in the sample CMC600.

1. Turbostratic structure of the boron nitride

Selected area diffraction of the remainind interphase is found in Figures 1, 2 and 3. The ring pattern is consistent with that of sp^2 -hybridised BN, and the diffuse rings indicate tBN. Some of the samples have uneven intensity of the rings that follow the curvature of the fibres, indicating a slight anisotropy with a preference for the sheets to aling along the fibre surface. The turbostratic nature of the interphase was confirmed by HR-TEM, see Figures 4, 5 and 6.

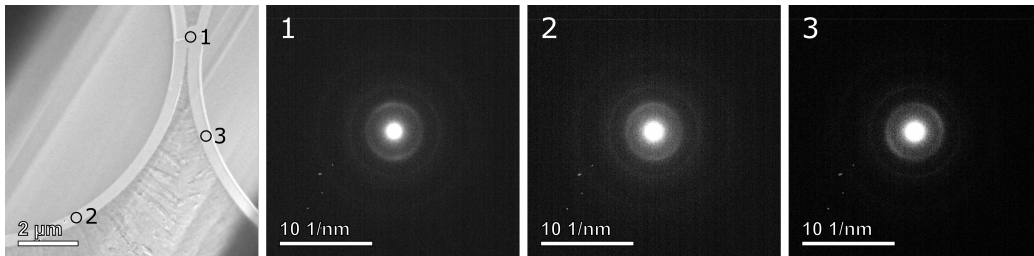


Figure 3: Diffraction patterns from the interphase in the sample CMC400.

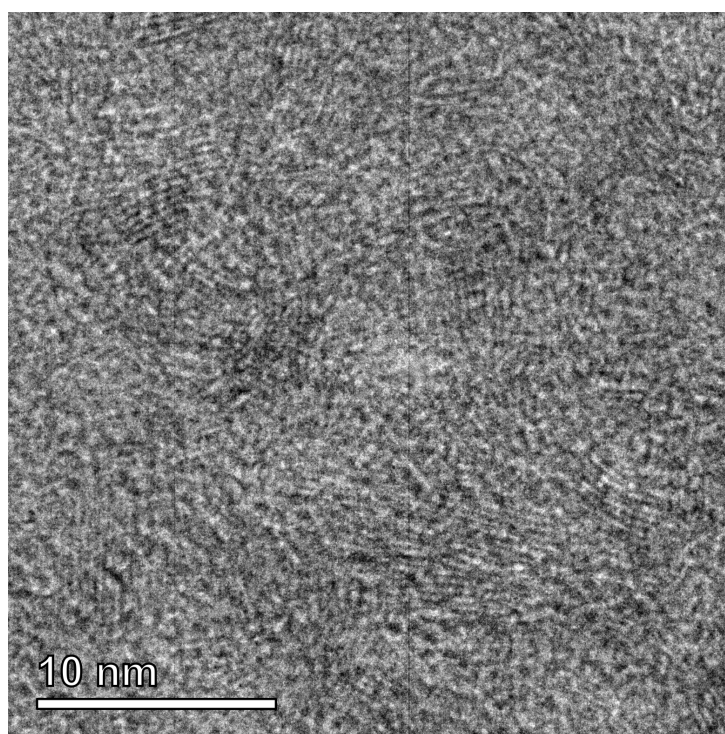


Figure 4: HR-TEM image of the interphase in the sample CMC1000.

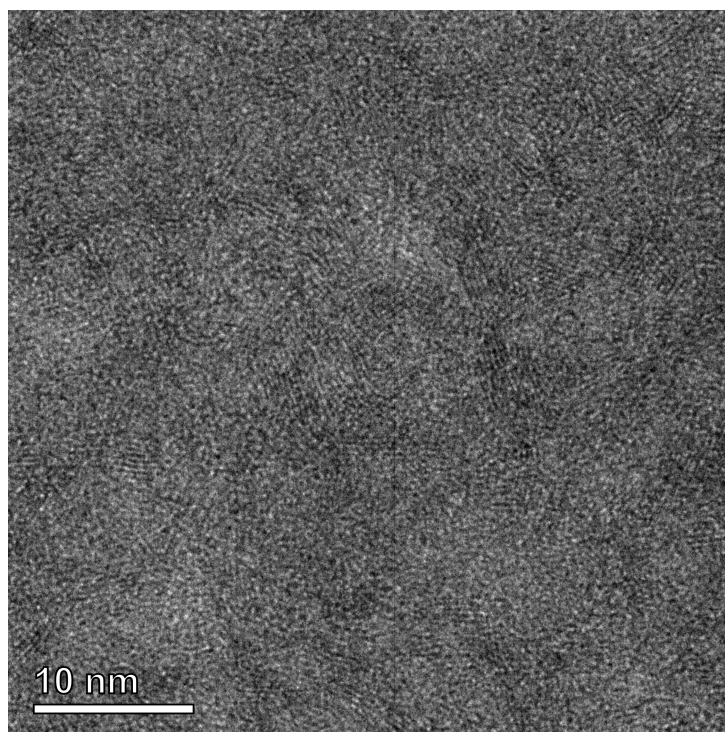


Figure 5: HR-TEM image of the interphase in the sample CMC600.

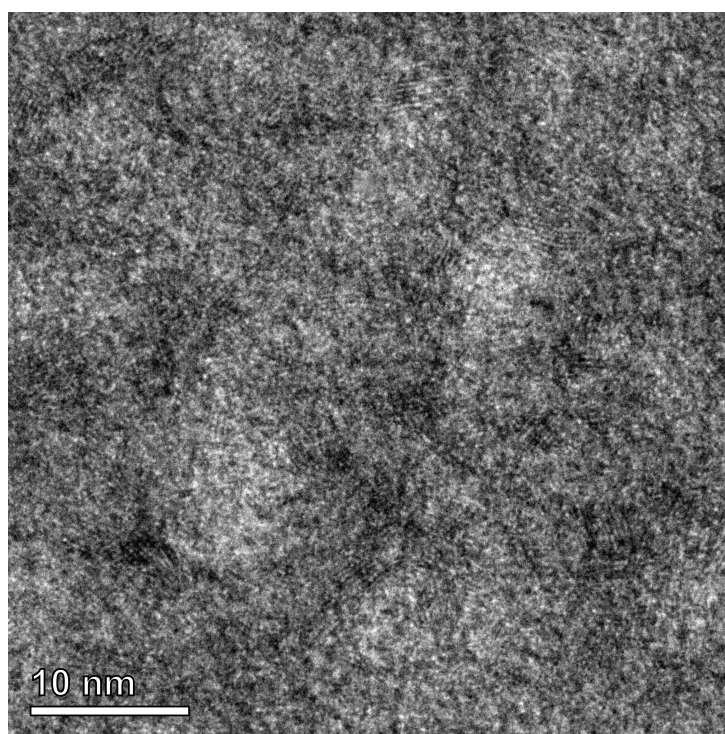


Figure 6: HR-TEM image of the interphase in the sample CMC400.

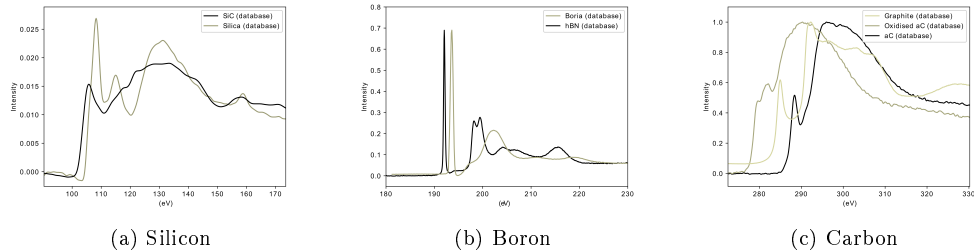


Figure 7: Silicon edges from database, α -silicon carbide and silica acquired by EELS. Boron edges from database, Hexagonal boron nitride acquired by EELS and boria acquired by XAS. Carbon edge from database, amorphous carbon, oxidised amorphous carbon and graphite acquired by EELS.

2. Database spectra

Identification of compounds was done by "fingerprinting" to database fine structure core loss spectra of relevant compounds, for the boron edge, data from hBN was used [1; 2] as the atomic orbital arrangement should be most similar to that of tBN, together with boria [2]. For silicon the reference spectra were those of α -SiC [3; 2] and amorphous silica [2]. For carbon data was compared to core loss spectra of amorphous carbon, oxidised amorphous carbon and graphite [4; 2]. All database spectra can be seen in Figure 7.

3. Additional elemental maps

3.1. CMC1000

Figure 8 shows elemental maps across CVI SiC/interphase/fibre from the CMC1000 surface sample, showing the presence of silica layers next to both CVI SiC and fibre.

3.2. CMC600

Figures 9 and 10 show the fibre surface with oxide layer as well as the CVI/interphase interface of sample CMC600, showing the presence of oxide on the fibre but not on the CVI SiC.

References

- [1] J. Verbeeck, S. Van Aert, G. Berton, Model-based quantification of eels spectra: Including the fine structure, *Ultramicroscopy* 106 (11-12) (2006) 976–980.

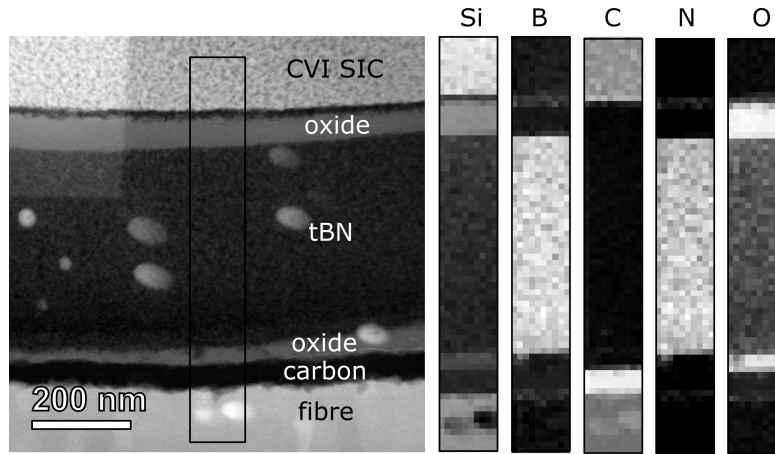


Figure 8: Elemental maps across the interphase of CMC1000 in the area between the two fibres. The dots are contamination from parking the electron beam during alignments.

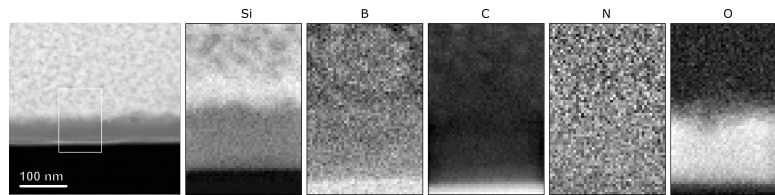


Figure 9: Elemental maps across the edge of the fibre in CMC600.

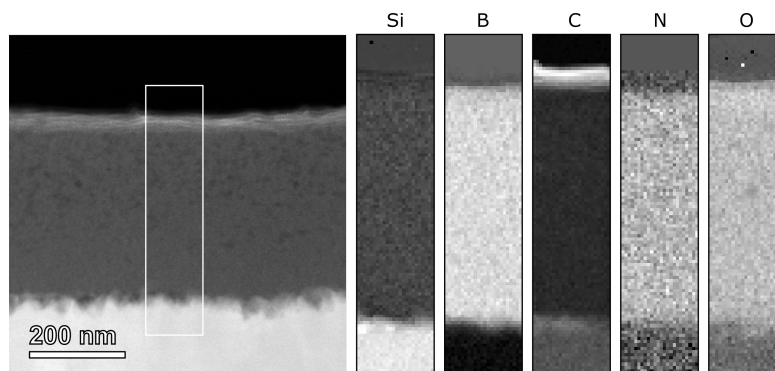


Figure 10: Elemental maps across the CVI/interphase interface in CMC600.

- [2] P. Ewels, T. Sikora, V. Serin, C. P. Ewels, L. Lajaunie, A complete overhaul of the electron energy-loss spectroscopy and x-ray absorption spectroscopy database: eelsdb.eu, *Microscopy and Microanalysis FirstView* (2016) 1–8. doi:10.1017/S1431927616000179.
URL <http://journals.cambridge.org/articles/1431927616000179>
- [3] W. Skiff, R. Carpenter, S.-H. Lin, Si 1 core edge fine structure in an oxidation series of silicon compounds: a comparison of microelectron energy loss spectra with theory, *Journal of applied physics* 58 (9) (1985) 3463–3469.
- [4] L. Lajaunie, C. Pardanaud, C. Martin, P. Puech, C. Hu, M. Biggs, R. Arenal, Advanced spectroscopic analyses on a: Ch materials: Revisiting the eels characterization and its coupling with multi-wavelength raman spectroscopy, *Carbon* 112 (2017) 149–161.